Daily, seasonal, and annual relationships between air and subsurface temperatures

Jason E. Smerdon,[1] Henry N. Pollack,[2] Vladimir Cermak,[3] John W. Enz,[4] Milan Kresl,[3] Jan Safanda,[3] and John F. Wehmiller[5]

Received 5 November 2004; revised 8 March 2005; accepted 18 January 2006; published 4 April 2006.

[1] Inversions of borehole temperature profiles that reconstruct past ground surface temperature (GST) changes have been used to estimate historical changes in surface air temperature (SAT). Paleoclimatic interpretations of GST reconstructions are based on the assumption that GST and SAT changes are closely coupled over decades, centuries, and longer. This assumption has been the subject of some debate because of known differences between GST and SAT at timescales of hours, days, seasons, and years. We investigate GST and SAT relationships on daily, seasonal, and annual timescales to identify and characterize the principal meteorological changes that lead to short-term differences between GST and SAT and consider the effects of those differences on coupling between the two temperatures over much longer time periods. We use observational SAT and subsurface data from Fargo, North Dakota; Prague, Czech Republic; Cape Henlopen State Park, Delaware; and Cape Hatteras National Seashore, North Carolina. These records comprise intradaily observations that span parts of one or two decades. We compare subsurface temperature observations to calculations from a conductive subsurface model driven with daily SAT as the surface boundary condition and show that daily differences exist between observed and modeled subsurface temperatures. We also analyze year-to-year spectral decompositions of daily SAT and subsurface temperature time series and show that dissimilarities between mean annual GST and SAT are attributable to differences in annual amplitudes of the two temperature signals. The seasonal partitioning of these amplitude differences varies from year to year and from site to site, responding to variable evapotranspiration and cryogenic effects. Variable year-to-year differences between mean annual GST and SAT are closely estimated using results from a multivariate regression model that associates the partial influences of seasonal meteorological conditions with the attenuation of annual GST amplitudes.

Citation: Smerdon, J. E., H. N. Pollack, V. Cermak, J. W. Enz, M. Kresl, J. Safanda, and J. F. Wehmiller (2006), Daily, seasonal, and annual relationships between air and subsurface temperatures, *J. Geophys. Res.*, *111*, D07101, doi:10.1029/2004JD005578.

1. Introduction

[2] Borehole temperature profiles have been used by many investigators to reconstruct global and hemispheric changes in ground surface temperature (GST) on timescales of centuries and longer [*Huang et al.*, 2000; *Harris and Chapman*, 2001; *Beltrami*, 2002]. These reconstructions have been interpreted as good estimates of changes in surface air temperature (SAT) and therefore have been used as representations of SAT changes at times prior to a widely developed instrumental SAT record. Such an interpretation is based on the assumption that GST and SAT are closely coupled on long timescales, i.e., decadal, centennial and longer. This assumption has become the subject of some discussion, however, because of known differences between GST and SAT on much shorter timescales spanning days, seasons and years [e.g., *Goodrich*, 1982; *Wehmiller et al.*, 2000; *Zhang et al.*, 2001; *Schmidt et al.*, 2001; *Kane et al.*, 2001; *Sokratov and Barry*, 2002; *Lin et al.*, 2003; *Stieglitz et al.*, 2003; *Beltrami and Kellman*, 2003; *Smerdon et al.*, 2003, 2004]. Differences also exist between hemispheric paleoclimate reconstructions derived from borehole temperature inversions and those derived from traditional proxy records of SAT [*Huang et al.*, 2000; *Briffa and Osborn*, 2002; *Mann et al.*, 2003; *Huang*, 2004; *Jones and Mann*, 2004; *Pollack and Smerdon*, 2004; *Esper et al.*, 2004], although some recent comparisons demonstrate improved agreement

[1]Lamont-Doherty Earth Observatory, Columbia University, Palisades, New York, USA.
[2]Department of Geological Sciences, University of Michigan, Ann Arbor, Michigan, USA.
[3]Geophysical Institute, Czech Academy of Sciences, Prague, Czech Republic.
[4]Department of Soil Science, North Dakota State University, Fargo, North Dakota, USA.
[5]Department of Geology, University of Delaware, Newark, Delaware, USA.

0148-0227/06/2004JD005578

[*Esper et al.*, 2002; *Moberg et al.*, 2005]. It therefore is important to understand the origin of differences between the various reconstructions of past climate, in part by examining the assumptions that underpin each reconstruction method. Here we investigate coupling between GST and SAT signals, thereby addressing issues relevant to borehole-based reconstructions of paleoclimate.

[3] The assumption that GST and SAT are coupled, on long or short timescales, has typically been investigated using three related and complementary approaches: (1) comparison of the temporal and spatial variation in collections of GST reconstructions with direct measurements of SAT during their period of overlap [e.g., *Lachenbruch and Marshall*, 1986; *Chisholm and Chapman*, 1992; *Beltrami et al.*, 1992; *Bodri and Cermak*, 1995, 1997; *Gosnold et al.*, 1997; *Harris and Gosnold*, 1999; *Huang et al.*, 2000; *Beltrami and Harris*, 2001; *Harris and Chapman*, 2001; *Beltrami*, 2002; *Roy et al.*, 2002; *Beltrami et al.*, 2003; *Pollack et al.*, 2003; *Mann et al.*, 2003; *Pollack and Smerdon*, 2004; *Majorowicz and Safanda*, 2005]; (2) model studies that include or parameterize the relevant physical, chemical and biological processes at the ground surface and enable controlled simulations of air and subsurface interactions [e.g., *Lin et al.*, 2003; *Mann and Schmidt*, 2003; *Stieglitz et al.*, 2003; *González-Rouco et al.*, 2003, 2006; *Chapman et al.*, 2004; *Schmidt and Mann*, 2004; *Bartlett et al.*, 2004, 2005]; and (3) empirical studies at site-specific locations using time series measurements of subsurface temperatures and meteorological conditions [e.g., *Baker and Ruschy*, 1993; *Osterkamp and Romanovsky*, 1994; *Beltrami*, 1996; *Putnam and Chapman*, 1996; *Zhang et al.*, 1997; *Beltrami and Harris*, 2001; *Beltrami*, 2001; *Zhang et al.*, 2001; *Schmidt et al.*, 2001; *Baker and Baker*, 2002; *Smerdon et al.*, 2003, 2004; *Beltrami and Kellman*, 2003].

[4] Assimilating the results of these studies is difficult because they generally fall into two distinct categories: They either represent short-term site-specific studies of subsurface temperatures and meteorological conditions or they comprise long-term regional comparisons between GST reconstructions and SAT records. The conclusions of these studies can therefore offer seemingly contradictory conclusions. On long timescales, GST reconstructions have been shown to reflect SAT histories, although ensembles of borehole temperature profiles are necessary to enhance the signal-to-noise ratio in reconstructions at all spatial scales [*Shen et al.*, 1995; *Beltrami et al.*, 1997; *Harris and Chapman*, 2001; *Pollack and Smerdon*, 2004]. On short timescales, however, meteorological and related hydrological processes, most notably evapotranspiration and the cryogenic effects associated with snow and the freezing and thawing of subsurface regimes, can cause hourly, daily, seasonal and annual differences between GST and SAT [e.g., *Kane et al.*, 2001; *Sokratov and Barry*, 2002; *Stieglitz et al.*, 2003; *Beltrami and Kellman*, 2003; *Smerdon et al.*, 2003, 2004]. Comparisons between air and ground temperatures at these various timescales are complicated by the fact that the magnitude and variability of differences between mean annual GST and SAT can be on the order of several kelvins at a given site, while long-term trends in the two temperatures are typically an order of magnitude smaller. It therefore remains a challenge to connect assessments of GST and SAT relationships on short timescales with assessments of the two temperatures over much longer timescales.

[5] Understanding short- and long-term coupling between GST and SAT requires that the factors influencing the coupling be understood in both a temporal and spatial context. The temporal aspect of this understanding is required because short-term differences between GST and SAT alone do not invalidate the assumption of long-term tracking of the two temperatures. Only secular changes in the short-term differences would weaken GST reconstructions as estimates of SAT history. If indeed these secular changes existed, their spatial distribution must also be considered because regional GST reconstructions comprise either joint inversions of spatially distributed boreholes [*Beltrami et al.*, 1997] or averaging of individual site-specific GST reconstructions [*Shen et al.*, 1995; *Pollack and Smerdon*, 2004].

[6] Here we establish a method for characterizing site-specific GST and SAT on short timescales in a manner that allows our results to be easily extended to broader spatial regions and longer timescales. We use observational data from Fargo, North Dakota; Prague, Czech Republic; Cape Henlopen State Park, Delaware; and Cape Hatteras National Seashore, North Carolina, all sites where high-resolution observations of air and subsurface temperatures have been collected over several years. These four data sets allow us to (1) identify the principal meteorological influences on daily, seasonal and annual differences between GST and SAT and to quantify the magnitude of those influences on a year-to-year basis, (2) develop insights into how differences between GST and SAT vary between several sites in variable climates and therefore give our results spatial context, and (3) demonstrate that the analytic methods we employ represent a simple way of characterizing seasonal and annual coupling between GST and SAT that enable an assessment of long-term tracking between the two temperatures. Taken collectively, our results help construct a regional picture of the variable effects that meteorological conditions can have on differences between GST and SAT on seasonal and annual timescales and provide a new method for understanding the short-term and long-term coupling of GST and SAT.

2. Data

[7] Observational data were collected at Fargo, North Dakota (46°54′N, 96°48′W); Prague, Czech Republic (50°02.5′N, 14°28.7′E); Cape Henlopen State Park, Delaware (38°46.4′N, 75°5.7′W) and Cape Hatteras National Seashore, North Carolina (35°15′N, 75°32′W). These four data sets comprise several years of relatively continuous measurements taken many meters into the subsurface at many observational depths. Such characteristics make them particularly suitable for demonstrating the analytical methods and conceptual framework that we seek to develop for use on a much broader scale. The data sets and measurement techniques have been described in detail by various authors [*Schmidt et al.*, 2001; *Wehmiller et al.*, 2000; *Smerdon et al.*, 2003, 2004]. A tabular summary of general information about each site is given by *Smerdon et al.* [2004].

Table 1. General Meteorological Conditions at the Observational Sites

Site	SAT Annual Mean,[a] °C	SAT Annual Range, °C	Mean Annual Rain-Equivalent Precipitation,[a] cm	Mean Annual Snowfall,[a] cm	Mean Annual Snow Cover,[a] days
Fargo, North Dakota	5.8 (81–89, 91, 93–98)	∼−35 to 35	52 (81–94, 97–99)	123 (81–95, 97–99)	96 (81–95)
Prague, Czech Republic	9.9 (1996, 1998–2001)	∼−10 to 25	53 (1990–2002)	31 (1990–2002)	35 (1990–2002)
Cape Henlopen, Delaware	15.0 (1998–2001)	∼−5 to 30	115 (1996–2001)	31 (1996–2000)	not available
Cape Hatteras, North Carolina	18.1 (1997–2001)	∼0 to 30	112 (1996, 1999, 2001)	0 (1996–2001)	0 (1996–2001)

[a]Numbers given in parentheses are the years used to calculate the annual means shown.

[8] Table 1 displays the principal meteorological information for the four sites during each period for which subsurface observations exist. This information does not necessarily characterize long-term meteorological normals at the sites, but represents the actual conditions during the periods of time that we investigate air and ground temperature relationships. Fargo experienced the coldest mean annual SAT (5.8°C) and coldest minimum winter temperatures (−30° to −40°C) during the period of record at the site. Prague registered warmer mean annual SAT (9.9°C) and less extreme winter minimums (−5° to −15°C). Both Fargo and Prague observed approximately the same amount of mean annual rain-equivalent precipitation (52 and 53 cm) but different cumulative annual snowfall during their respective periods of observation. At Fargo and Prague the mean annual snowfall was 123 and 31 cm and the mean number of days each year with snow cover in excess of 2.5 cm was 96 and 35 days, respectively. Capes Henlopen and Hatteras are considerably warmer sites, with respectively 15.0°C and 18.1°C mean annual SAT. Neither Cape Henlopen nor Cape Hatteras experienced significant periods of time during which SAT was below 0°C, and both sites experienced over twice as much mean-annual precipitation as Fargo or Prague. Little or no precipitation fell as snow at the two sites during their periods of record (the mean snowfall determined from the 5 years of snowfall data at Cape Henlopen is significantly affected by one large snowfall year; the yearly cumulative snowfalls between 1996 and 2000 were 116.5, 2.5, 0, 7.4 and 27.7 cm). We highlight these meteorological differences to emphasize that the four data sets comprise observations in several climatic settings, with site-to-site variations in snow cover, ground freezing, precipitation, and SAT that provide a range of conditions under which to characterize the influence of meteorological conditions on GST and SAT coupling.

3. Daily, Seasonal, and Annual Relationships Between Observed and Modeled Subsurface Temperatures

3.1. Observational Data

[9] Figures 1–3 display 2 contrasting years of observational data from Fargo, 2 years from Prague, and 1 year each from Cape Henlopen and Cape Hatteras. The upper panel in each figure displays daily rain-equivalent precipitation and daily snow cover. Daily SAT for each year is plotted in the second panel from the top. Observed subsurface temperatures at Fargo, Prague, Cape Henlopen, and Cape Hatteras are displayed over the depth ranges 0.01–4.7 m, 0.0–5.0 m, 0.25–3.0 m and 0.1–3.0 m, respectively. All plots in Figures 1–3 employ the same temperature contour interval. To isolate effects in full summer and winter seasons we split calendar years into seasonal years, i.e., years that contain a full summer and a full winter. Fargo observed the longest duration of snow cover into the spring, and no snowfall occurred there after April during any of the years on record. We therefore begin each seasonal year on 1 May and use this convention for all locations.

[10] The foremost characteristic of Figures 1–3 is their visual representation of the differences between the conditions at the four sites. Fargo is the coldest location, while Capes Henlopen and Hatteras display the warmest temperatures. The Prague observations, shown in Figure 2, reflect intermediate conditions. Differences in the amount and frequency of precipitation at each site are also clearly highlighted in the upper panels of Figures 1–3. These upper panels also clearly demonstrate the difference in the amount and duration of snow cover at the four sites, which ranges from tens of centimeters of snow cover throughout the duration of the winter at Fargo to an absence of snow at the Cape Henlopen site.

[11] In addition to underscoring the climatic differences between the sites, the years displayed in Figures 1–3 have also been chosen to demonstrate the variable influence of meteorological conditions on subsurface temperatures. Both pairs of years in Figures 1 and 2 are representative of different winter extremes. Figure 1 displays measurements from the heaviest and lightest snow years during the period of observation at Fargo. During the 1981–1982 winter, cumulative snowfall totaled 177 cm and the ground was covered by at least 2.5 cm of snow for 115 days, while the corresponding observations during the 1982–1983 winter were 59 cm and 32 days. Figure 2 presents the equivalent pairing of years from Prague. During the 1996–1997 (heaviest snow year) and 1999–2000 (lightest snow year) winters, the respective cumulative snowfalls totaled 35 and 31 cm, and the ground was covered by 2.5 cm of snow for 60 and 13 days. Figure 3 presents the 1999–2000 year at Capes Henlopen and Hatteras. Neither of these two sites experienced periods of snow cover during the 1999–2000 winter, while both sites observed significantly greater total precipitation than Fargo or Prague. Capes Henlopen and Hatteras therefore provide examples of precipitation effects on subsurface temperatures in noncryogenic regions, and provide insightful contrasts to the Fargo and Prague observations.

3.2. Conductively Modeled Subsurface Temperatures

[12] In addition to the observational data shown in Figures 1–3, we also display subsurface temperatures calculated with a conductive model driven by daily SAT as the surface boundary condition. The model calculates subsurface temperatures as a function of time using the analytic solution of the one-dimensional heat conduction

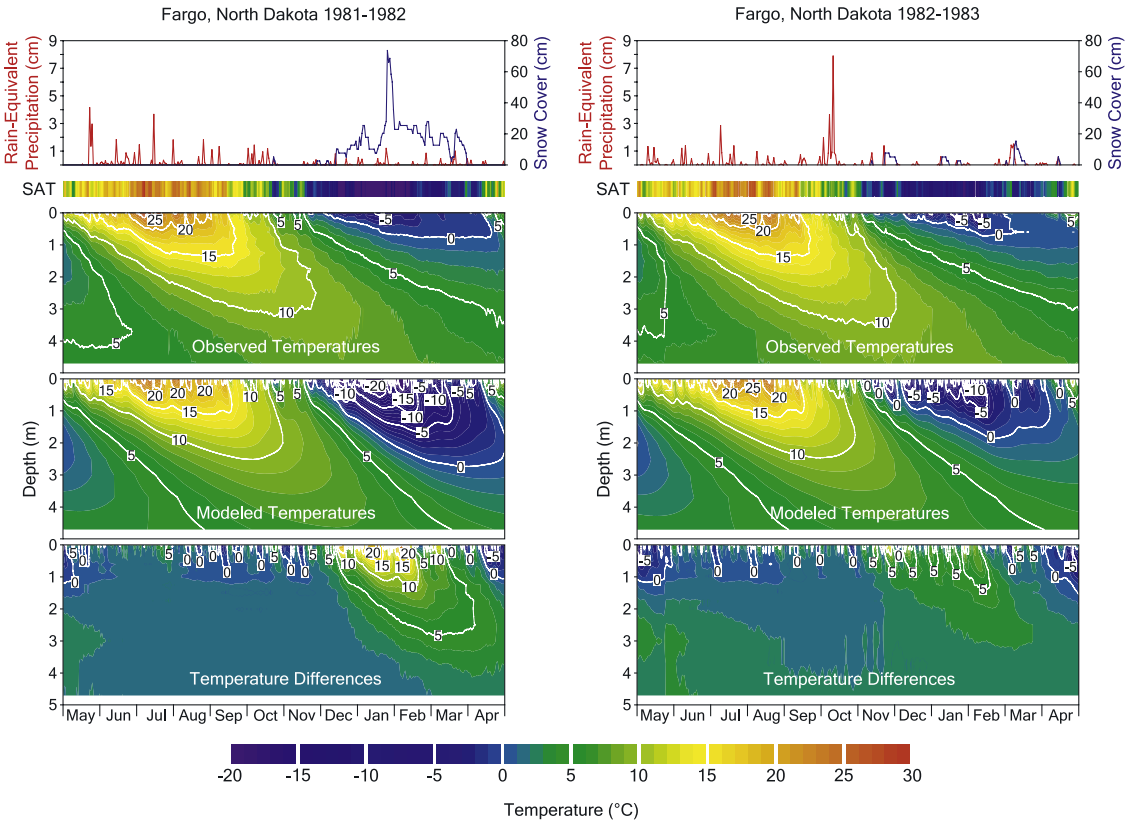

Figure 1. Observed and modeled data at Fargo, North Dakota, during the seasonal years 1981–1982 and 1982–1983. The upper panels display daily rain-equivalent precipitation and snow cover (total rain-equivalent precipitation, accumulative snowfall, and total snow cover days in 1981–1982 and 1982–1983 were 49 and 51 cm, 117 and 59 cm, and 115 and 32 days, respectively). Panels second from the top display daily SAT. Observed subsurface temperatures are plotted between the depths 0.01 and 4.7 m. Conductively modeled subsurface temperatures, using SAT as the surface driving function, are plotted at depths equal to observational depths. Lower panels display observed and modeled temperature differences (observed minus modeled temperatures). All plots employ the same contour intervals, and solid white areas denote depths where temperatures are not plotted.

equation for a surface boundary condition composed of step changes [*Carslaw and Jaeger*, 1959]. For a surface temperature history comprising N time steps of equal duration, the temperature at a time t_N and depth z is given as

$$T(z, t_N) = T_0 + \sum_{i=1}^{N} \Delta T_i \, \mathrm{erfc}\left(\frac{z}{\sqrt{4\kappa i \Delta t}}\right), \qquad (1)$$

where ΔT_i is the surface temperature change of the ith step,

$$t_N = \sum_{i=1}^{N} i\Delta t,$$

κ is the thermal diffusivity of the medium and Δt is the time step interval. The subsurface is assumed to be homogeneous with an initial uniform temperature T_0; as indicated by equation (1), cryogenic effects are not modeled in this formalism. We display only selected years from each multiyear time series, but subsurface temperatures for the entire periods of observation were calculated using a spin-up of 2 years at the beginning of each record. For thermal diffusivity we use the average thermal diffusivities estimated by *Smerdon et al.* [2003, 2004] at each of the sites. These estimated diffusivities at Fargo, Prague, Cape Henlopen and Cape Hatteras are $0.37 \pm 0.01 \times 10^{-6}$ m^2 s^{-1}, $0.65 \pm 0.05 \times 10^{-6}$ m^2 s^{-1}, $0.94 \pm 0.09 \times 10^{-6}$ m^2 s^{-1} and $1.04 \pm 0.05 \times 10^{-6}$ m^2 s^{-1}, respectively.

3.3. Comparisons Between Observed and Modeled Daily Temperatures

[13] Comparison between observed and modeled temperatures in Figures 1–3 shows that the observational subsurface temperatures display the gross features of a conductive subsurface driven by SAT. Seasonal SAT extremes are muted with depth as the amplitudes of the annual signals are attenuated. High-frequency fluctuations with periods of days or weeks are quickly attenuated and are effectively absent below the uppermost several tens of centimeters. A progressive smoothing of daily temperature variations with depth is the visible result. A phase lag with depth is also clear, as temperature changes occur later in the year at deeper depths, i.e., maximum summer temperatures at the surface do not cause changes at depth until days or months later. Differences between observational and modeled data are also evident, however, and we explore these differences in the sections that follow.

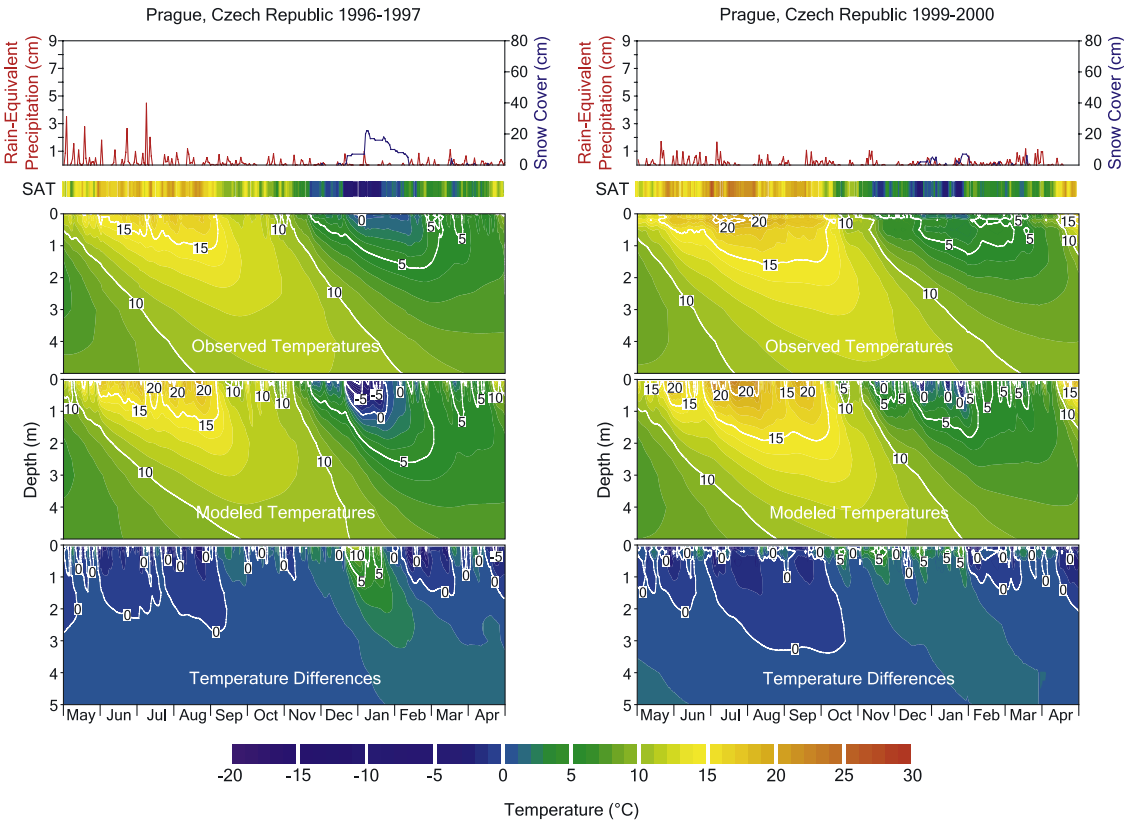

Figure 2. Observed and modeled data at Prague, Czech Republic, during the seasonal years 1996–1997 and 1999–2000. The upper panels display daily rain-equivalent precipitation and snow cover (total rain-equivalent precipitation, accumulative snowfall, and total snow cover days in 1996–1997 and 1999–2000 were 59 and 46 cm, 35 and 31 cm, and 60 and 13 days, respectively). Panels second from the top display daily SAT. Observed subsurface temperatures are plotted between the depths 0.0 and 5.0 m. Conductively modeled subsurface temperatures, using SAT as the surface driving function, are plotted at depths equal to observational depths. Lower panels display observed and modeled temperature differences (observed minus modeled temperatures). All plots employ the same contour intervals.

3.3.1. Daily Differences

[14] At Fargo and Prague, observed daily temperatures in the subsurface are not as cold as modeled temperatures during much of the winter. These differences are particularly evident during the heavy snow years in Figures 1 and 2. The differences are also larger at Fargo than those at Prague, the winters at the former site being more extreme than at the latter. Effects due to latent heat of freezing are also visible in the observational data, particularly in Figure 1, where a "zero-curtain" isotherm [*Outcalt et al.*, 1990] is reached in the upper meter and maintained throughout much of the winter. This latent energy is also important during the spring melt when colder temperatures are maintained later in the subsurface than those generated with the conductive model, because latent heat is absorbed by the frozen subsurface layers and delays the warming at greater depths. This is evidenced by negative temperature differences during late winter and early spring months in both Figures 1 and 2. In contrast to the relatively large winter differences between observed and modeled temperatures at Fargo and Prague, both Cape Henlopen and Cape Hatteras, where no significant cryogenic processes occur, display differences between observed and modeled temperatures that are very close to zero, much smaller than at Fargo and Prague.

[15] In the summer, daily differences between observed and modeled temperatures are evident at Capes Henlopen and Hatteras and to a lesser extent at Prague. During much of the summer and early fall, measured subsurface temperatures are colder than the modeled temperatures, as evidenced by the negative differences in Figures 2 and 3. These colder temperatures, present several meters below the surface, are likely maintained by diminished heat fluxes into the subsurface buffered by evapotranspiration, effectively yielding cooler subsurface temperature maxima during the summer relative to model calculations. Particularly at Capes Henlopen and Hatteras, temperature differences persist for several months during the summer and penetrate to several meters depth. Advective transport of heat by precipitation also is important in the evolution of shallow subsurface temperatures. With regard to seasonal and annual temperature relationships between the air and subsurface, however, evapotransporation is likely more significant because of its persistence throughout the summer season; advective heat transport by precipitation, while it has the potential to cause high-amplitude changes to subsurface temperatures during precipitation events, is likely an ephemeral effect within the context of seasonal and annual air and subsurface temperature relationships.

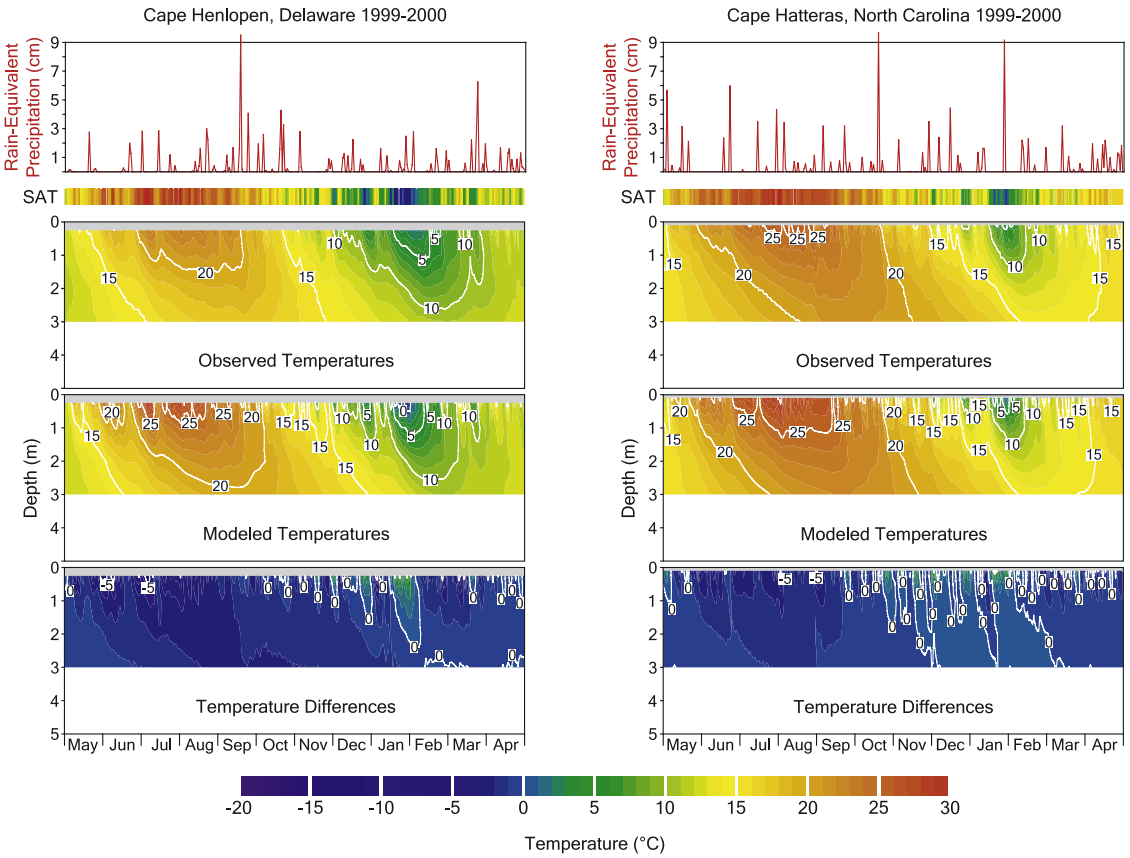

Figure 3. Observed and modeled data at Cape Henlopen State Park, Delaware, and Cape Hatteras National Seashore, North Carolina, during the seasonal year 1999–2000. The upper panels display daily rain-equivalent precipitation at the two sites (total rain-equivalent precipitation at Cape Henlopen and Cape Hatteras was 107 and 127 cm, while no significant snow cover was observed). Panels second from the top display daily SAT. Observed subsurface temperatures are plotted between the depths 0.25 and 3.0 m at Cape Henlopen and 0.1 and 3.0 m at Cape Hatteras. Conductively modeled subsurface temperatures, using SAT as the surface driving function, are plotted at depths equal to observational depths. Lower panels display observed and modeled temperature differences (observed minus modeled temperatures). All plots employ the same contour intervals, and solid white areas denote depths where temperatures are not plotted.

3.3.2. Seasonal Differences

[16] Figures 1–3 display daily differences between observed and modeled temperatures, but they also highlight seasonal differences, manifest as large tongues of temperature difference throughout portions of the years at each site. To illustrate further the seasonal differences between observed temperatures and those derived from a conductive model driven with a SAT boundary condition, we plot in Figure 4 the differences between observed and modeled temperatures at 1-m depth for 4 years at each site, effectively a single depth slice from the 1-year contour plots of Figures 1–3, yet spanning more time. With the exception of the 1996–1997 year at Prague, each year from Figures 1–3 is contained in the data displayed in Figure 4. These time series are smoothed using 21-day moving averages to filter high-frequency fluctuations and allow persistent seasonal differences between measured and modeled temperatures at 1-m depth to emerge more clearly.

[17] Figure 4 complements Figures 1–3 by displaying seasonal differences between observed and modeled temperatures, as well as site-to-site variability in the magnitude of these differences; Fargo experiences the largest differences in winter, while Capes Henlopen and Hatteras have the largest differences in summer. More notably, however, Figure 4 clearly illustrates the year-to-year variability in the magnitude of seasonal differences. These differences, if they showed secular trends, would represent a degradation of the idealized stationary coupling scenario underpinning GST reconstructions as representations of historical SAT. The timescale represented in Figure 4 is much too short, however, to directly address the presence of secular trends. We therefore focus the remainder of our attention on how such differences affect comparisons of SAT and reconstructed GST signals on a year-to-year and site-to-site basis, with the purpose of gaining insight into the coupling between the two temperatures over longer timescales.

4. GST and SAT Comparisons

4.1. Year-to-Year Annual GST and SAT Signals

[18] *Smerdon et al.* [2003, 2004] have quantified seasonal differences between GST and SAT using amplitude and

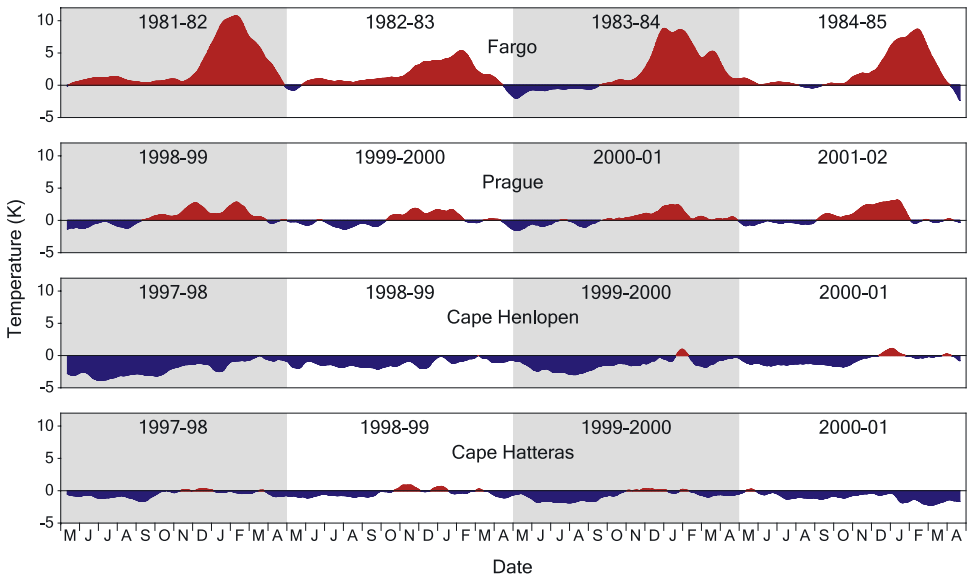

Figure 4. Differences at a depth of 1 m between observed subsurface temperatures and conductively modeled subsurface temperatures driven by SAT as the surface boundary condition. Four seasonal years of data are displayed, each year beginning on 1 May. All time series have been smoothed with a 21-day moving filter.

phase relationships between annual GST and SAT signals at each of the four sites presented here. They extract an average annual signal from the multiyear periods of observation at each location. Our objective here, however, is to reconstruct variable year-to-year GST signals from subsurface temperature observations. It therefore is necessary to modify the *Smerdon et al.* [2003] analysis to account for phase shifts with depth in subsurface temperature time series; surface temperature changes during a May-to-April seasonal year will cause changes in subsurface temperatures at progressively later periods of time with depth.

[19] We account for phase shifts by analyzing the daily subsurface time series in yearly time windows that are shifted forward in time, relative to segments of SAT beginning on 1 May of each year. The analyzed window is forward shifted at each depth by the estimates of average phase shifts determined from analyses of the entire observational periods at the sites [*Smerdon et al.*, 2003, 2004]. The Fourier component with annual period is extracted from each year-to-year segment at each depth. The year-to-year amplitude of the annual GST signal is then estimated by extrapolating subsurface amplitudes to the ground surface using a least squares linear regression of the natural log of the subsurface amplitudes, in accordance with the analytic solution of the one-dimensional diffusion equation [*Carslaw and Jaeger*, 1959].

[20] In Figures 5–8 we plot the reconstructions of annual GST signals. Each year-to-year annual signal has been referenced to the seasonal year mean of the shallowest observations at each site. Also shown in Figures 5–8 are yearly extractions of annual SAT signals, referenced to their own seasonal year means. We do not reconstruct years where large gaps in the records occur, such as in the Fargo data during 1990 and 1992, and the Prague data during 1997. Because of phase shifts, these gaps comprise progressive losses of information from the previous year at increasing depths. Therefore, in addition to 1990–1991 and 1992–1993, we do not reconstruct the 1989–1990 and 1991–1992 years at Fargo; we exclude only the 1997–1998 year from the Prague analysis because the position and length of the gap in that year does not result in significant information losses in the previous seasonal year. These considerations are reflected in the missing reconstructed years in Figures 5 and 6. We also plot the percent difference between annual GST and SAT amplitudes in the lower panels of Figures 5–8.

[21] Differences between year-to-year amplitudes of annual GST and SAT signals range from 13.7 to 36.4%, 9.6 to 15.6%, 5.9 to 15.7% and −2.3 to 12.9% at Fargo, Prague, Cape Henlopen and Cape Hatteras, respectively; the average amplitude differences for the full period of observation at the four sites are respectively 22.5 ± 0.7, 12.6 ± 1.5, 8.3 ± 3.9 and 7.6 ± 2.0% [*Smerdon et al.*, 2003, 2004] and are denoted as dashed lines in the lower panels of Figures 5–8. The spatial distribution of these amplitude differences confirms what we have earlier identified as the dominant meteorological effects at each site (see section 3). Fargo displays significantly more decoupling between GST and SAT amplitudes in the winter than in the summer. Relative to Fargo, winter amplitude differences between GST and SAT are smaller at Prague and reflect the reduced winter effects at the site. In contrast to Fargo and Prague, Capes Henlopen and Hatteras experience decoupling that is predominantly concentrated in the summer seasons.

4.2. Association of GST Amplitude Differences With Seasonal Meteorological Conditions

[22] The year-to-year estimates of annual GST and SAT signals shown in Figures 5–8 allow a quantification of the influence of seasonal meteorological conditions on amplitude differences between the two temperatures. This quantification requires two assumptions: (1) cooler subsurface

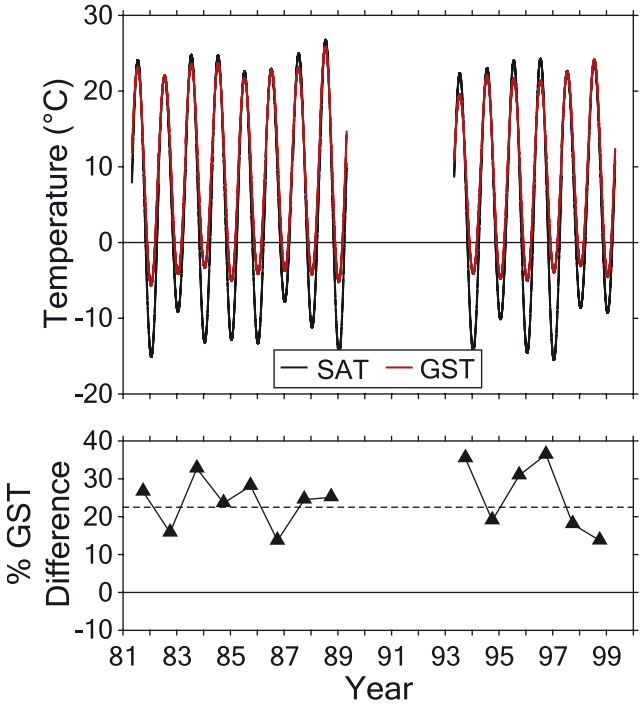

Figure 5. Upper panel displays year-to-year annual signals determined for each seasonal year in the SAT and reconstructed GST at Fargo, North Dakota. Lower panel displays the year-to-year percent difference between the amplitudes of the two signals. The dashed line denotes the average percent difference during the entire period of record.

temperatures in summer are dependent on the amount of summer precipitation and the energy available to drive evapotranspiration (i.e., peak warmth during summer months; see *Lin et al.* [2003] for an extensive discussion); and (2) warmer subsurface temperatures in winter are dependent on the number of snow cover days and the severity of cold air temperatures from which the subsurface is insulated. In other words, as the product of summer precipitation and summer warmth increases so should the relative difference between peak summer SAT and GST, and as the product of snow cover days and winter temperatures decrease the difference between peak winter SAT and GST should increase. Accordingly, we perform a multivariate-linear regression,

$$GST_{Difference} = \alpha(P \times SAT_{JJA}) + \beta(SCD \times SAT_{DJF}) + \in, \quad (2)$$

where $GST_{Difference}$ is the year-to-year percent differences of the annual GST signal relative to the SAT, P is the cumulative precipitation in months without snow during a seasonal year; SAT_{JJA} is the mean SAT during June, July and August; SCD is the total number of snow cover days (days in which snow cover in excess of 2.5 cm was observed) during a seasonal year; and SAT_{DJF} is the mean SAT during December, January, and February. The term $\in$ is an assumed error term with white noise characteristics. The predictors and predictand are standardized prior to regression.

[23] We illustrate the application of the multivariate-regression model using the Fargo data. Between the seasonal years of 1981–1982 and 1997–1998 at Fargo there are 10 years for which all necessary observations are available. The regression analysis yields $\alpha = 0.39 \pm 0.11$ and $\beta = -1.06 \pm 0.11$, values that are significant at the $p = 1.0 \times 10^{-2}$ and 3.3×10^{-5} levels, respectively. The two predictors explain 91% of the total variance (adjusted r^2; all variances described hereinafter are based on the adjusted r^2 estimate) in the percent differences of the annual GST signal, significant at the $p = 1.1 \times 10^{-4}$ level. These results support the concept that meteorological conditions, as we have framed them, are the dominant influences on differences between GST and SAT and lend validity to the seasonal model that we have proposed.

[24] No other combination or separation of the predictors given in equation (2), including additional regression terms, explains the variance in percent GST attenuation as completely. SCD alone explains 67% of the variance in GST attenuation, significant at the $p = 2.2 \times 10^{-3}$ level. If the product of SCD and SAT_{DJF} is used as a single predictor, 77% of the variance in GST attenuation is explained, significant at the $p = 0.5 \times 10^{-3}$ level. The parallel correlation analyses using P and SAT_{JJA} explain relatively little of the variance in annual GST attenuation, with little statistical significance. Once again, these results suggest that, at Fargo, winter effects are the dominant meteorological influences on GST differences, relative to SAT. Nevertheless, the regression model employing both winter and

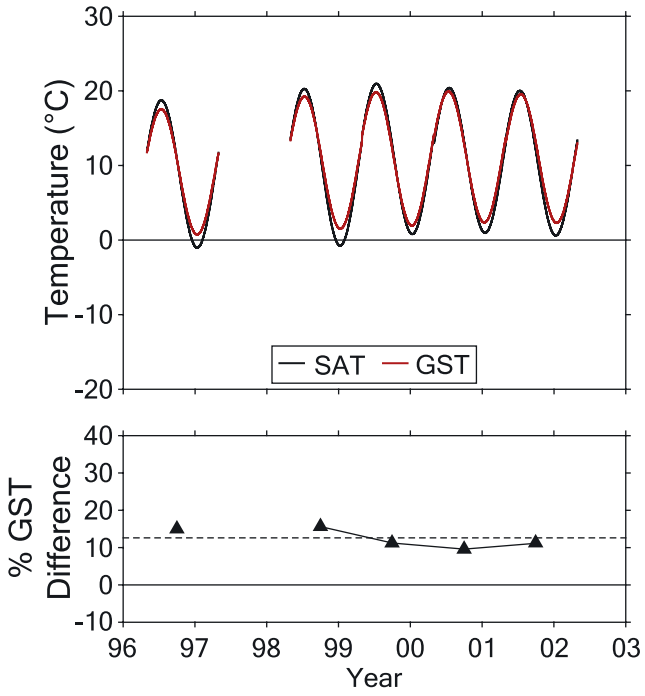

Figure 6. Upper panel displays year-to-year annual signals determined for each seasonal year in the SAT and reconstructed GST at Prague, Czech Republic. Lower panel displays the year-to-year percent difference between the amplitudes of the two signals. The dashed line denotes the average percent difference during the entire period of record.

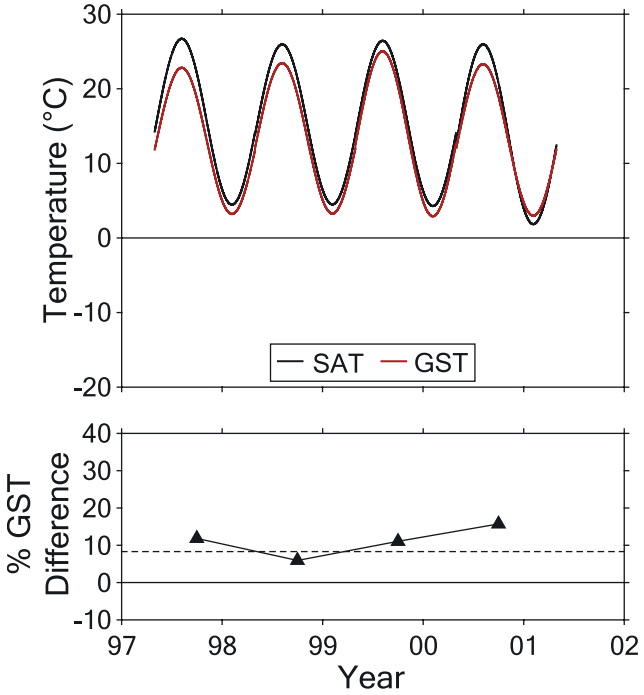

Figure 7. Upper panel displays year-to-year annual signals determined for each seasonal year in the SAT and reconstructed GST at Cape Henlopen State Park, Delaware. Lower panel displays the year-to-year percent difference between the amplitudes of the two signals. The dashed line denotes the average percent difference during the entire period of record.

summer effects explains more variance at a higher statistical significance than any single variable and is the most physically justified representation of the processes that affect air and subsurface coupling at Fargo during a full seasonal year. This full-year approach to analyzing differences between GST and SAT further underscores the importance of including both summer and winter effects in the assessment of annual GST and SAT coupling [*González-Rouco et al.*, 2003; *Chapman et al.*, 2004; *Smerdon et al.*, 2004]. Additional verification of the multivariate-regression model proposed here, or variants thereof, will require application of the model to many more sites in various climatic settings over longer timescales. While we have presented three other data sets in this study, these records comprise too few degrees of freedom to establish regression results with sufficient statistical significance.

4.3. Calculating Differences Between Mean Annual GST and SAT Using Amplitude Relationships

[25] The amplitude characterization method presented in section 4.1 provides an effective means by which to characterize GST signals from subsurface temperature time series, and the regression analysis presented in section 4.2 suggests that the principal differences between GST and SAT amplitudes can be explained in terms of seasonal meteorological conditions. Differences between mean annual GST and SAT can be calculated by combining the results of sections 4.1 and 4.2, and allow annual temperature means, the most common quantity used to track differences between GST and SAT, to be directly addressed.

[26] If the principal seasonal differences between GST and SAT can be captured as amplitude decoupling in summer and/or winter, then the consequences for mean annual values of GST are straightforward. For instance, attenuation during the summer will reduce mean annual GST relative to SAT, while attenuation during the winter will cause mean annual GST to increase relative to SAT. More generally, the quantitative difference between the full-period mean of a harmonic signal and the mean of the same signal that has been reduced or increased at its maximum or minimum is

$$\overline{\mathrm{GST}}_{\mathrm{annual}} - \overline{\mathrm{SAT}}_{\mathrm{annual}} = \left(\frac{\mathrm{GST}_{\mathrm{SPA}} - \mathrm{SAT}_{\mathrm{SPA}}}{2}\right) + \left(\frac{\mathrm{GST}_{\mathrm{WPA}} - \mathrm{SAT}_{\mathrm{WPA}}}{2}\right), \quad (3)$$

where $\mathrm{GST}_{\mathrm{SPA}}$, $\mathrm{GST}_{\mathrm{WPA}}$, $\mathrm{SAT}_{\mathrm{SPA}}$, and $\mathrm{SAT}_{\mathrm{WPA}}$ are the summer peak amplitudes and winter peak amplitudes of the annual GST and SAT signals, respectively, and $\overline{\mathrm{GST}}_{\mathrm{annual}} - \overline{\mathrm{SAT}}_{\mathrm{annual}}$ is the difference between mean annual GST and SAT in a seasonal year. In terms of the quantities used in this study, including the regression coefficients from equation (2), equation (3) can be written

$$\overline{\mathrm{GST}}_{\mathrm{annual}} - \overline{\mathrm{SAT}}_{\mathrm{annual}} = -\alpha\left(\mathrm{SAT}_{\mathrm{Amplitude}} \times \mathrm{GST}_{\mathrm{Difference}}\right) + |\beta|\left(\mathrm{SAT}_{\mathrm{Amplitude}} \times \mathrm{GST}_{\mathrm{Difference}}\right), \quad (4)$$

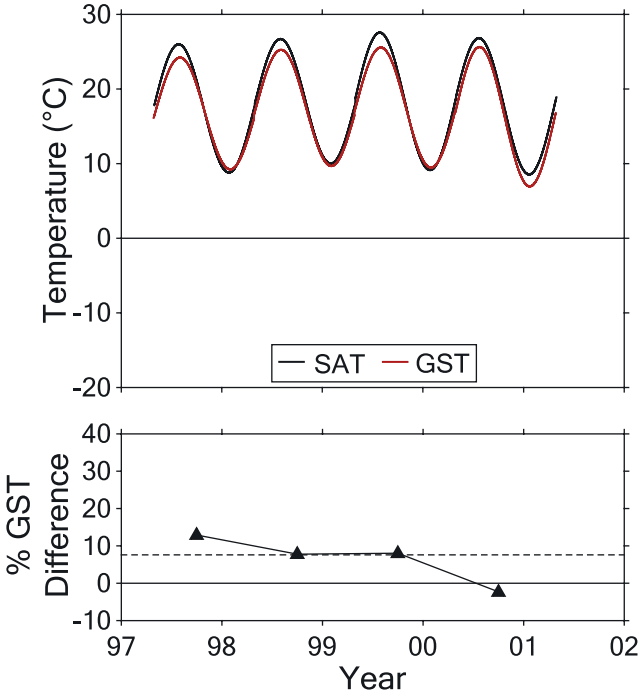

Figure 8. Upper panel displays year-to-year annual signals determined for each seasonal year in the SAT and reconstructed GST at Cape Hatteras National Seashore, North Carolina. Lower panel displays the year-to-year percent difference between the amplitudes of the two signals. The dashed line denotes the average percent difference during the entire period of record.

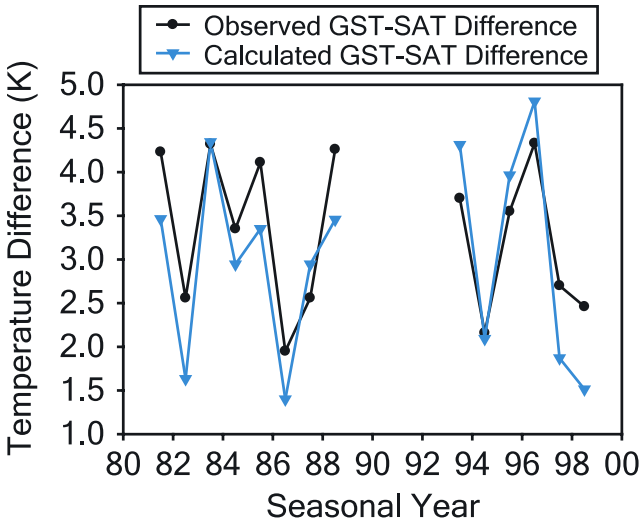

Figure 9. Measured and calculated mean annual GST-SAT differences at Fargo, North Dakota, between the 1981–1982 and 1998–1999 seasonal years.

where $SAT_{Amplitude}$ is the year-to-year amplitude of the annual SAT signal.

[27] The observed differences between the mean annual GST and SAT and the calculated differences using the amplitude characterization given in equation (4) are shown for Fargo in Figure 9. Calculated differences explain 73% of the variance in the observed differences. This corresponds to a linear correlation between observed and calculated temperature differences of 0.86, significant at the $p < 0.0001$ level. Neither of the differences, measured or calculated, have a significant linear trend over the roughly two decades of time represented in Figure 9. These results suggest that we have captured the gross features of the differences between GST and SAT differences, and that the method has potential as a means of investigating these differences in the context of long-term changes in seasonal meteorological conditions. These results are, of course, only representative of Fargo, but the correspondence between observed and calculated temperature differences provides support for two aspects of the analytic methods that we have developed: (1) most of the seasonal temperature differences between GST and SAT can be well captured using the spectral characterization of temperature time series that we have employed; and (2) seasonal decoupling, occurring primarily during the summer and winter, establishes the principal differences between mean annual GST and SAT.

5. Discussion

[28] We have already noted that annual differences between GST and SAT, such as those displayed in Figure 9, do not alone imply that GST and SAT are decoupled over long timescales. Studies must ultimately track annual GST and SAT coupling over much longer timescales to determine if long-term increases or decreases in annual differences exist. This conclusion is underscored by the fact that the magnitude and variability of differences between mean annual GST and SAT can be on the order of several kelvins at a given site, while long-term trends in the two temperatures are typically on the order of several tenths of a kelvin per century. If relationships between GST and SAT are assessed over only a few years, their long-term behavior will therefore be obscured by the large interannual differences between the two temperatures.

[29] This study has also offered a way to quantitatively characterize the influence of meteorological conditions on the difference between mean annual GST and SAT. Tracking changes in precipitation and snow cover has the potential to offer insight into how GST and SAT relationships may have changed in time. The influence of such changes, however, must be further explored. Locations outside of midlatitude regions may experience effects different from those that we have observed at the four midlatitude sites investigated here. At high latitudes, cryogenic effects are extensive and exist throughout most of the year. In such regions, the thawing and freezing of permafrost in the short active season [e.g., *Zhang et al.*, 1997; *Hinkel et al.*, 2001] may mute the significance of evapotranspiration during the summer. Snow cover is also present for large portions of the year and may not be separated easily into winter half-years as we have done here.

[30] The magnitude of latent energy fluxes is also dependent on the hydrologic characteristics of the subsurface. The extent to which moisture penetrates and is stored in the subsurface will be determined by the porosity and permeability of subsurface media. This, in turn, will influence the magnitude of latent energy fluxes driven by freezing, thawing and evapotranspiration. Areas with low porosity and permeability will not be significantly affected by these processes, and therefore annual differences between GST and SAT may not be strongly partitioned into seasons. Evapotranspiration also may become increasingly important year round at low-latitude sites. Capes Henlopen and Hatteras illustrate how moisture fluxes out of the subsurface cool the ground during the winter. This presumably will become more pronounced at lower latitudes where year-round solar radiation is greater.

6. Conclusions

[31] We have assessed differences between observed subsurface temperatures and conductively modeled subsurface temperatures driven by SAT as a surface boundary condition. Observed temperatures are different from modeled temperatures in summer and winter seasons by amounts that are consistent with the dominant meteorological conditions present at the four observational sites. These differences are ultimately manifest as differences between GST and SAT that can be effectively quantified by spectrally decomposing temperature time series into year-to-year annual signals.

[32] Observed spatial variations in the seasonal partitioning of differences between annual amplitudes of GST and SAT signals support the hypothesis that summer evapotranspiration and winter cryogenic effects are the dominant meteorological conditions causing differences between the two temperatures. Additionally, the observed differences between annual GST and SAT can be closely approximated using daily meteorological observations. This implies that annual GST-SAT differences can be effectively estimated with only meteorological information. Given very long

meteorological records, calculations of GST-SAT differences over many decades are therefore possible, and potential trends in these differences can be investigated. The techniques developed in this study thus represent an analytical framework with which to examine the tracking of GST and SAT changes over long timescales and broad spatial regions.

[33] **Acknowledgments.** We thank the staff of Cape Henlopen State Park (Delaware) and Cape Hatteras National Seashore (North Carolina) for permission to obtain data at these sites. We also gratefully acknowledge H. A. Stecher III and Linda L. York for their technical assistance. This research was supported in part by NSF award ATM-0081864 and NASA grant GWEC 0000 0132 to the University of Michigan, by NSF award EAR9315052 to the University of Delaware, by GACR grant 205/03/0998 to the Geophysical Institute of the Czech Academy of Sciences, and by the Office of the Vice President for Research of the University of Michigan. J. E. Smerdon was additionally supported by a Lamont-Doherty Postdoctoral Fellowship from the Lamont-Doherty Earth Observatory of Columbia University.

References

Baker, D. G., and D. L. Ruschy (1993), The recent warming in eastern Minnesota shown by ground temperatures, *Geophys. Res. Lett.*, *20*, 371–374.

Baker, J. M., and D. G. Baker (2002), Long-term ground heat flux and heat storage at a mid-latitude site, *Clim. Change*, *54*, 295–303.

Bartlett, M. G., D. S. Chapman, and R. N. Harris (2004), Snow and the ground temperature record of climate change, *J. Geophys. Res.*, *109*, F04008, doi:10.1029/2004JF000224.

Bartlett, M. G., D. S. Chapman, and R. N. Harris (2005), Snow effect on North American ground temperatures, 1950–2002, *J. Geophys. Res.*, *110*, F03008, doi:10.1029/2005JF000293.

Beltrami, H. (1996), Active layer distortion of annual air/soil thermal orbits, *Permafrost Periglacial Processes*, *7*, 101–110.

Beltrami, H. (2001), On the relationship between ground temperature histories and meteorological records: A report on the Pomquet station, *Global Planet. Change*, *29*, 327–348.

Beltrami, H. (2002), Climate from borehole data: Energy fluxes and temperatures since 1500, *Geophys. Res. Lett.*, *29*(23), 2111, doi:10.1029/2002GL015702.

Beltrami, H., and R. N. Harris (Eds.) (2001), Inference of climate change from geothermal data, *Global Planet. Change*, *29*, 148–352.

Beltrami, H., and L. Kellman (2003), An examination of short- and long-term air-ground temperature coupling, *Global Planet. Change*, *38*, 291–303.

Beltrami, H., A. M. Jessop, and J. C. Mareschal (1992), Ground temperature histories in eastern and central Canada from geothermal measurements: Evidence of climatic change, *Palaeogeogr. Palaeoclimatol. Palaeoecol.*, *98*, 167–184.

Beltrami, H., L. Z. Cheng, and J.-C. Maraschal (1997), Simultaneous inversion of borehole temperature data for past climate determination, *Geophys. J. Int.*, *129*, 311–318.

Beltrami, H., C. Gosselin, and J. C. Mareschal (2003), Ground surface temperatures in Canada: Spatial and temporal variability, *Geophys. Res. Lett.*, *30*(10), 1499, doi:10.1029/2003GL017144.

Bodri, L., and V. Cermak (1995), Climate changes of the last millennium inferred from borehole temperatures: Results from the Czech Republic: Part I, *Global Planet. Change*, *11*, 111–123.

Bodri, L., and V. Cermak (1997), Climate changes of the last millennium inferred from borehole temperatures: Results from the Czech Republic: Part II, *Global Planet. Change*, *14*, 163–173.

Briffa, K. R., and T. J. Osborn (2002), Blowing hot and cold, *Science*, *295*, 2227–2228.

Carslaw, H. S., and J. C. Jaeger (1959), *Conduction of Heat in Solids*, 2nd ed., 510 pp., Oxford Univ. Press, New York.

Chapman, D. S., M. G. Bartlett, and R. N. Harris (2004), Comment on "Ground vs. surface air temperature trends: Implications for borehole surface temperature reconstructions" by M. E. Mann and G. Schmidt, *Geophys. Res. Lett.*, *31*, L07205, doi:10.1029/2003GL019054.

Chisholm, T., and D. S. Chapman (1992), Climate change inferred from analysis of borehole temperatures: An example from western Utah, *J. Geophys. Res.*, *97*, 14,155–14,177.

Esper, J., E. R. Cook, and F. H. Schweingruber (2002), Low-frequency signals in long tree-line chronologies for reconstructing past temperature variability, *Science*, *295*, 2250–2253.

Esper, J., D. C. Frank, and R. J. S. Wilson (2004), Climate reconstructions: Low frequency ambition and high frequency ratification, *Eos Trans. AGU*, *85*(12), 120, 113.

González-Rouco, F., H. von Storch, and E. Zorita (2003), Deep soil temperature as proxy for surface air-temperature in a coupled model simulation of the last thousand years, *Geophys. Res. Lett.*, *30*(21), 2116, doi:10.1029/2003GL018264.

González-Rouco, J. F., H. Beltrami, E. Zorita, and H. von Storch (2006), Simulation and inversion of borehole temperature profiles in surrogate climates: Spatial distribution and surface coupling, *Geophys. Res. Lett.*, *33*, L01703, doi:10.1029/2005GL024693.

Goodrich, L. E. (1982), The influence of snow cover on the ground thermal regime, *Can. Geotech. J.*, *19*, 421–432.

Gosnold, W. D., P. E. Todhunter, and W. Schmidt (1997), The borehole temperature record of climate warming in the mid-continent of North America, *Global Planet. Change*, *15*, 33–45.

Harris, R. N., and D. S. Chapman (2001), Mid-latitude (30°–60°) climatic warming inferred by combining borehole temperatures with surface air temperatures, *Geophys. Res. Lett.*, *28*, 747–750.

Harris, R. N., and W. D. Gosnold (1999), Comparisons of borehole temperature-depth profiles and surface air temperatures in the northern plains of the USA, *Geophys. J. Int.*, *138*, 541–548.

Hinkel, K. M., F. Paetzold, F. E. Nelson, and J. G. Bockheim (2001), Patterns of soil temperature and moisture in the active layer and upper permafrost at Barrow, Alaska: 1993–1999, *Global Planet. Change*, *29*, 293–309.

Huang, S. (2004), Merging information from different resources for new insights into climate change in the past and future, *Geophys. Res. Lett.*, *31*, L13205, doi:10.1029/2004GL019781.

Huang, S., H. N. Pollack, and P. Y. Shen (2000), Temperature trends over the last five centuries reconstructed from borehole temperatures, *Nature*, *403*, 756–758.

Jones, P. D., and M. E. Mann (2004), Climate over past millennia, *Rev. Geophys.*, *42*, RG2002, doi:10.1029/2003RG000143.

Kane, D. L., K. M. Hinkel, D. J. Goering, L. D. Hinzman, and S. I. Outcalt (2001), Non-conductive heat transfer associated with frozen soils, *Global Planet. Change.*, *29*, 275–292.

Lachenbruch, A. H., and B. V. Marshall (1986), Climate change: Geothermal evidence from permafrost in the Alaskan Arctic, *Science*, *234*, 689–696.

Lin, X., J. E. Smerdon, A. W. England, and H. N. Pollack (2003), A model study of the effects of climatic precipitation changes on ground temperatures, *J. Geophys. Res.*, *108*(D7), 4230, doi:10.1029/2002JD002878.

Majorowicz, J., and J. Safanda (2005), Measured versus simulated transients of temperature logs: A test of borehole climatology, *J. Geophys. Eng.*, *2*(4), 291–298.

Mann, M. E., and G. A. Schmidt (2003), Ground vs. surface air temperature trends: Implications for borehole surface temperature reconstructions, *Geophys. Res. Lett.*, *30*(12), 1607, doi:10.1029/2003GL017170.

Mann, M. E., S. Rutherford, R. S. Bradley, M. K. Hughes, and F. T. Keiming (2003), Optimal surface temperature reconstructions using terrestrial borehole data, *J. Geophys. Res.*, *108*(D7), 4203, doi:10.1029/2002JD002532. (Correction, *J. Geophys. Res.*, *109*, D11107, doi:10.1029/2003JD004290, 2004.)

Moberg, A., D. M. Sonechkin, K. Holmgren, N. M. Datsenko, and W. Karlén (2005), Highly variable northern hemisphere temperatures reconstructed from low- and high-resolution proxy data, *Nature*, *433*, 613–617.

Osterkamp, T. E., and V. E. Romanovsky (1994), Characteristics of changing permafrost temperatures in the Alaskan arctic, USA, *Arct. Alp. Res.*, *28*, 267–273.

Outcalt, S. I., F. E. Nelson, and K. M. Hinkel (1990), The zero-curtain effect: Heat and mass transfer across an isothermal region in freezing soil, *Water Resour. Res.*, *26*(7), 1509–1516.

Pollack, H. N., and J. E. Smerdon (2004), Borehole climate reconstructions: Spatial structure and hemispheric averages, *J. Geophys. Res.*, *109*, D11106, doi:10.1029/2003JD004163.

Pollack, H. N., D. Y. Demezhko, A. D. Duchkov, I. V. Golovanova, S. Huang, V. A. Shchapov, and J. E. Smerdon (2003), Surface temperature trends in Russia over the past five centuries reconstructed from borehole temperatures, *J. Geophys. Res.*, *108*(B4), 2180, doi:10.1029/2002JB002154.

Putnam, S. N., and D. S. Chapman (1996), A geothermal climate change observatory: First year results from Emigrant Pass in northwest Utah, *J. Geophys. Res.*, *101*, 21,877–21,890.

Roy, S., R. N. Harris, R. U. M. Rao, and D. S. Chapman (2002), Climate change in India inferred from geothermal observations, *J. Geophys. Res.*, *107*(B7), 2138, doi:10.1029/2001JB000536.

Schmidt, G. A., and M. E. Mann (2004), Reply to comment by D. Chapman et al. on "Ground vs. surface air temperature trends: Implications for

borehole surface temperature reconstructions", *Geophys. Res. Lett.*, *31*, L07206, doi:10.1029/2003GL019144.

Schmidt, W. L., W. D. Gosnold, and J. W. Enz (2001), A decade of air-ground temperature exchange from Fargo, North Dakota, *Global Planet. Change*, *29*, 311–325.

Shen, P.-Y., H. N. Pollack, S. Huang, and K. Wang (1995), Effects of subsurface heterogeneity on the inference of climate change from borehole temperature data: Model studies and field examples from Canada, *J. Geophys. Res.*, *100*, 6383–6396.

Smerdon, J. E., H. N. Pollack, J. W. Enz, and M. J. Lewis (2003), Conduction-dominated heat transport of the annual temperature signal in soil, *J. Geophys. Res.*, *108*(B9), 2431, doi:10.1029/2002JB002351.

Smerdon, J. E., H. N. Pollack, V. Cermak, J. W. Enz, M. Kresl, J. Safanda, and J. F. Wehmiller (2004), Air-ground temperature coupling and subsurface propagation of annual temperature signals, *J. Geophys. Res.*, *109*, D21107, doi:10.1029/2004JD005056.

Sokratov, S. A., and R. G. Barry (2002), Intraseasonal variation in the thermoinsulation effect of snow cover on soil temperature and energy balance, *J. Geophys. Res.*, *107*(D10), 4093, doi:10.1029/2001JD000489.

Stieglitz, M., S. J. Dery, V. E. Romanovsky, and T. E. Osterkamp (2003), The role of snow cover in the warming of arctic permafrost, *Geophys. Res. Lett.*, *30*(13), 1721, doi:10.1029/2003GL017337.

Wehmiller, J. F., H. A. Stecher III, L. L. York, and I. Friedman (2000), The thermal environment of fossils: Effective ground temperatures (1994–1999) at aminostratigraphic sites, U. S. Atlantic coastal plain, in *Perspectives in Amino Acid and Protein Geochemistry*, edited by G. A. Goodfriend et al., pp. 219–250, Oxford Univ. Press, New York.

Zhang, T., T. E. Osterkamp, and K. Stamnes (1997), Effects of climate on active layer and permafrost on the North Slope of Alaska, *Permafrost Periglacial Processes*, *8*, 45–67.

Zhang, T., R. G. Barry, D. Gilichinsky, S. S. Bykhovets, V. A. Sorokovikov, and J. Ye (2001), An Amplified signal of climatic change in soil temperatures during the last century at Irkutsk, Russia, *Clim. Change*, *49*, 41–76.

V. Cermak, M. Kresl, and J. Safanda, Geophysical Institute, Czech Academy of Sciences, Bocni II/1401, 14131 Prague 4, Czech Republic.

J. W. Enz, Department of Soil Science, North Dakota State University, Walster Hall 106, P. O. Box 5638, Fargo, ND 58105-5638, USA.

H. N. Pollack, Department of Geological Sciences, University of Michigan, Ann Arbor, MI 48109, USA.

J. E. Smerdon, Lamont-Doherty Earth Observatory, Columbia University, P. O. Box 1000, 61 Route 9W, Palisades, NY 10964-1000, USA. (jsmerdon@ldeo.columbia.edu)

J. F. Wehmiller, Department of Geology, University of Delaware, Newark, DE 19716, USA.